Electrochemistry in Ultrahigh Vacuum: Underpotential Deposition of Al on Polycrystalline W and Au from Room Temperature $AlCl_3$/1-Ethyl-3-methylimidazolium Chloride Melts

Matthew Johnston,[†] Jae-Joon Lee,[§] Gary S. Chottiner,[‡] Barry Miller,[†] Tetsuya Tsuda,[||] Charles L. Hussey,[||] and Daniel A. Scherson*[,†]

Department of Chemistry, Case Western Reserve University, Cleveland, Ohio 44106, Departments of Physics, Case Western Reserve University, Cleveland, Ohio 44106, Department of Applied Chemistry, Konkuk University, Chungju, Korea, and Department of Chemistry and Biochemistry, The University of Mississippi, University, Mississippi 38677

Received: March 10, 2005; In Final Form: April 12, 2005

The voltammetric characteristics of polycrystalline Au and W electrodes cleaned (thermal annealing at 1100 K) and characterized (Auger electron spectroscopy) in ultrahigh vacuum (UHV) have been examined in ultrapure $AlCl_3$/1-ethyl-3-methylimidazolium chloride (EtMeImCl) melts in UHV. These experiments were performed using a custom-designed transfer system that allows for the all-Al electrochemical cell to be filled with EtMeImCl in an auxiliary UHV chamber and later transferred under UHV to the main UHV chamber that houses the Auger electron spectrometer. The results obtained for the underpotential (UPD) and bulk deposition of Al on Au were found to be very similar to those reported in the literature for measurements carried out under 1 atm of an inert gas in a glovebox. For the far more reactive W surfaces, voltammetric features ascribed to the stripping of underpotential-deposited Al could be observed following a single scan from 1.0 V vs Al^{3+}/Al to a potential negative enough for bulk deposition of Al to ensue. This behavior is unlike that reported in the literature for experiments performed in a glovebox, which required either extensive potential cycling in the Al bulk deposition and stripping region or excursions to potentials positive enough for chlorine evolution to ensue for Al UPD features to be clearly discerned. These observations open new prospects for fundamental electrochemical studies of well-characterized, highly reactive metals, including single crystals, in a variety of low vapor pressure ionic liquids.

Introduction

Room-temperature ionic liquids have emerged as a promising class of molten salts with application in a variety of technologically important areas.[1−4] Among their interesting properties is a wide liquid temperature range, typically 170−470 K, and negligible vapor pressure. Electrochemical applications of these solvents have centered on the possibility of electrodepositing Al and Al-based alloys from ambient temperature $AlCl_3$−RCl melts,[5−11] where R represents an asymmetric organic cation, with adjustable Lewis acidity and an ionic composition dependent on the $AlCl_3$:RCl molar ratio (N).[12] Our research efforts have focused on the fundamental aspects of underpotential (UPD) and bulk deposition of Al on Au and boron-doped diamond (BDD)[13] electrodes from $AlCl_3$/1-ethyl-3-methylimidazolium chloride ($AlCl_3$/EtMeImCl) molten salts at room temperature. In contrast to the behavior found for Au, W surfaces require conditioning, either extensive potential cycling in the Al bulk deposition and stripping[14] or excursions to potentials positive enough for chlorine evolution to ensue, i.e., 3 V vs Al^{3+}/Al in $AlCl_3$/EtMeImCl, for Al UPD voltammetric features to be identified. This phenomenon has been ascribed to the removal of oxide impurities adsorbed on the W surface, a procedure also found to decrease the overpotential needed to induce the bulk deposition of Al.[10]

This work examines the electrochemical behavior of W electrodes cleaned by heating in ultrahigh vacuum (UHV) at ca. 1100 K, a procedure that reduced the amount of oxygen (relative to W) on the surface to values of ca. 2%, as determined by Auger electron spectroscopy (AES). Various schemes have been described in the literature for electrochemical studies of well-defined electrode surfaces prepared and characterized in UHV involving aqueous electrolytes, which rely on ingenious systems that allow specimens to be transferred to a separate chamber, which is later isolated and filled with ca. 1 atm of an inert gas before introducing the electrolyte.[15−20] For the present work, we have taken advantage of the exceedingly low vapor pressure of $AlCl_3$/EtMeImCl melts, i.e., no detectable vaporization fragments at room temperature as determined by mass spectrometry (see below) within the pressure range attainable with our system, ca. 5×10^{-11} kPa, 0.133 kPa = 1 Torr, to perform conventional electrochemical experiments in the same UHV chamber that houses the surface analytical techniques. A closely related strategy was implemented earlier in our laboratory for studies of underpotential and bulk Li deposition on various surfaces in UHV from solid polymeric electrolytes, which also display negligible volatility.[21]

Experimental Section

All of the procedures involved in the preparation and execution of the experiments (except for the initial transfer of the melt to chamber III, see below) were performed in a multistage UHV system shown schematically in Figure 1. Chamber I consists of an ion-pumped bell jar (base pressure

* To whom correspondence may be addressed. E-mail: dxs16@po.cwru.edu.
[†] Department of Chemisty, Case Western Reserve University.
[‡] Department of Physics, Case Western Reserve University.
[§] Konkuk University.
[||] The University of Mississippi.

10.1021/jp051243m CCC: $30.25
Published on Web 05/13/2005

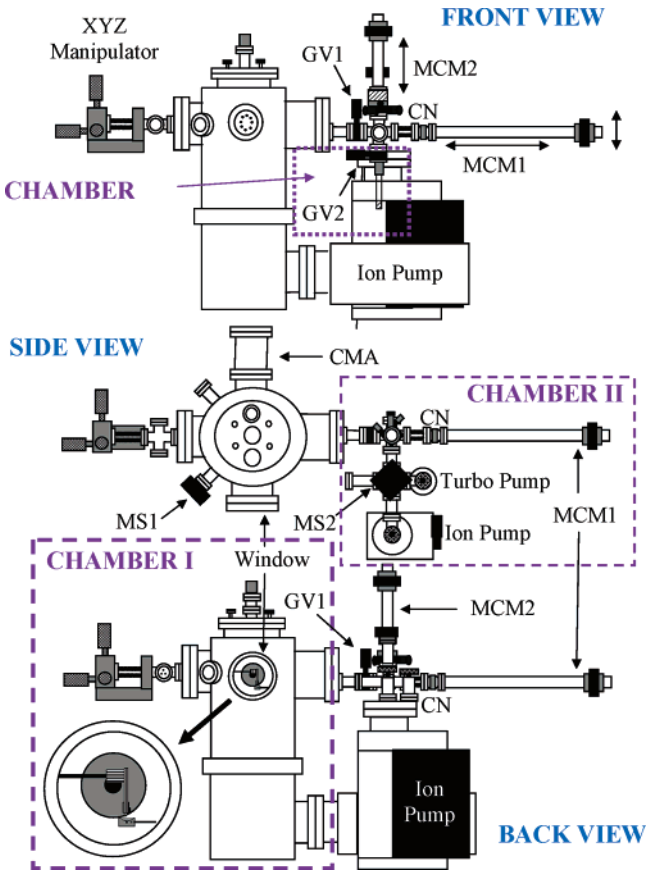

Figure 1. Schematic diagram of the UHV system involved in the preparation and spectroscopic and electrochemical characterization of electrodes in UHV. GV, gate valve; MCM, magnetically coupled manipulator; CN, ceramic nipple; MS, mass spectrometer.

ca. 5×10^{-11} kPa) equipped with a single-pass cylindrical mirror electron energy analyzer (CMA, Physical Electronics) for AES, a 2-keV ion gun for sputtering (Physical Electronics), a mass spectrometer (MS1, Ametek Dycor 2000) for monitoring continuously the composition of residual gases, and resistive sample heating capabilities (up to 1200 K). Au and W substrates were attached to the manually driven XYZ bellows manipulator shown in the figure. Electrolyte handling, including filling of the electrochemical cell (see below), is carried out in a separate, independently turbo-ion pumped UHV chamber denoted as II in Figure 1. This chamber is equipped with a second mass spectrometer (MS2, Ametek Dycor 2000) and two magnetically coupled manipulators, which are used to deliver electrolyte from chamber III to the electrochemical cell (MCM2) and to transfer the filled electrochemical cell from chamber II to chamber I (MCM1).

All of the data presented in this work were obtained with mirror-polished (using alumina powders, down to 0.05 μm) end surfaces of either Au or W rods with cross sectional (circular) areas of 0.28 and 0.32 cm^2, respectively, that were 10 mm in length. These substrates were rinsed thoroughly with ultrapure water and attached to ceramic tubes, which provide electrical isolation, and held in position by Ta heating wires. Following vapor degreasing with 2-propanol, the assemblies were mounted onto the Cu holder and affixed to the XYZ manipulator in the UHV system. Both Au and W surfaces were cleaned and characterized in Chamber I either by a series of sputter (1.5 keV Ar^+, current ca. 3−5 μA for 30 min.)/anneal (DC resistive heating, 50 A) cycles (for Au) or by a heat treatment at ca.

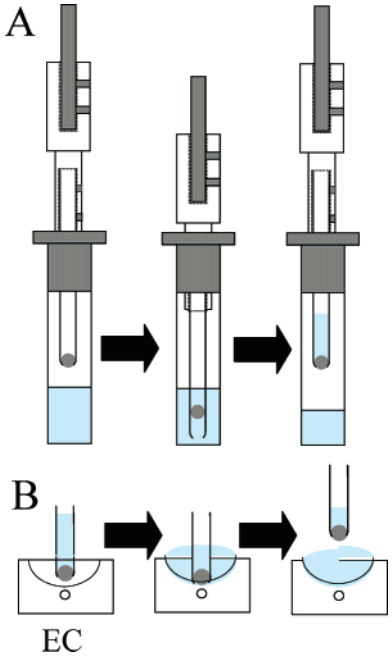

Figure 2. Schematic diagram of the sequence of steps involved in the filling of the tube with the ionic melt (panel A) and the delivery of the liquid to the electrochemical cell (EC, panel B, see text for details).

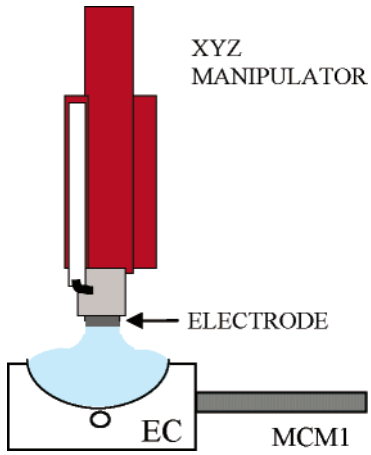

Figure 3. Schematic diagram showing the electrode/electrolyte in the hanging meniscus configuration.

1100 K (for W). In the case of Au, carbon impurities were removed by heating in oxygen at ca. 1.3×10^{-7} kPa.

Acidic ($N = 1.1$) $AlCl_3$/EtMeImCl melts were prepared at the University of Mississippi by methods described in detail elsewhere[22] and shipped to CWRU over coiled Al wire in sealed glass ampules. The contents were transferred to a UHV-compatible glass/metal flask (chamber III) in an Ar-filled glovebox (VAC), equipped with water and oxygen analyzers. Chamber III was then removed from the glovebox and attached to one of the ports of chamber II (see Figure 1) for thorough degassing. A few milliliters of the melt were transferred from chamber III using a tapered glass tube containing an enclosed glass ball to a concave shallow cavity machined into a high-purity Al block attached in turn to MCM1, which served as the electrochemical cell (EC, see B, Figure 2) and counter/reference (C/R) electrode during electrochemical measurements. As shown schematically in part A of Figure 2, immersion of the tube into the liquid displaces the ball upward allowing liquid to flow into the tube. Upon retrieval of the filled tube, the ball seals the end, trapping the liquid inside. The EC is then placed under

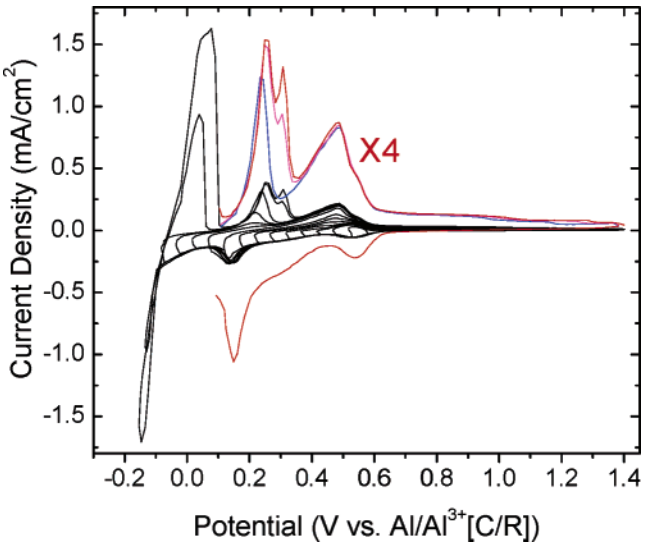

Figure 4. Series of voltammetric scans recorded at 20 mV/s for a Au electrode prepared and characterized in UHV in $AlCl_3$/EtMeImCl (N = 1.1, see text) recorded in UHV. The sequence was initiated from 1.4 V and reversing at progressively more negative potential values in 50-mV increments (only a few of these scans are displayed for clarity). Also shown in this figure in expanded form (X4) are the last three curves in this series in the sequence (blue, magenta, red) as well as one the corresponding curves recorded in the scan in the negative direction in the UPD range.

the tube as shown in part B of Figure 2 and carefully allowed to touch the bottom of the EC, thus displacing the ball upward causing the liquid to flow from the tube into the EC. At this stage, the tube is removed and the filled EC is transferred to chamber I and placed directly beneath the metal substrate. The liquid surface was first allowed to touch the surface of the AES-characterized electrode and then carefully retracted to form a hanging meniscus, see Figure 3. At this stage, the pressure in chamber I was typically on the order of 5×10^{-9} Torr with HCl as the major gas impurity detected in the mass spectrum.

Results and Discussion

Gold Electrode.

To assess the reliability of the instrumental array and experimental procedures, measurements were performed for Au surfaces prepared and characterized by the methods specified in the Experimental Section. Shown in Figure 4 are a series of voltammetric scans in the negative direction initiated at 1.4 V at a scan rate of 20 mV/s and reversed at progressively more negative potential values (window opening) in 50-mV increments. Both the shape and positions of all the features observed, particularly those associated with the UPD of Al, are virtually identical to those reported earlier for measurements performed in a high-quality glovebox.[17,18] For clarity, the current axis of the last three scans in the positive direction in this series was expanded in the UPD stripping region (X4). Also shown in this figure, for completeness, is one of the corresponding curves recorded in the scan in the negative direction. The assignment of each of these peaks has been discussed in detail in a previous paper and will not be repeated here. On this basis, it can be concluded that the methods described herein can be used with confidence for electrochemical studies involving other more reactive metals such as tungsten.

Tungsten Electrode.

For these experiments, the W surface was heated at ca. 1100 K for 16 h, yielding only C (268 eV, 4%) and O (500 eV, 2%) as detectable impurities with AES *just prior to contacting the $AlCl_3$/EtMeImCl melt electrolyte at room temperature in UHV*. Immediately after the hanging meniscus was formed, the first cycle was initiated at 1.0 V and reversed at 0.6 V vs Al^{3+}/Al at 20 mV/s. For all other subsequent cycles, the negative limit was extended in sequence toward more negative values in steps of 0.05 V down to −0.15 V, keeping the upper limit fixed at

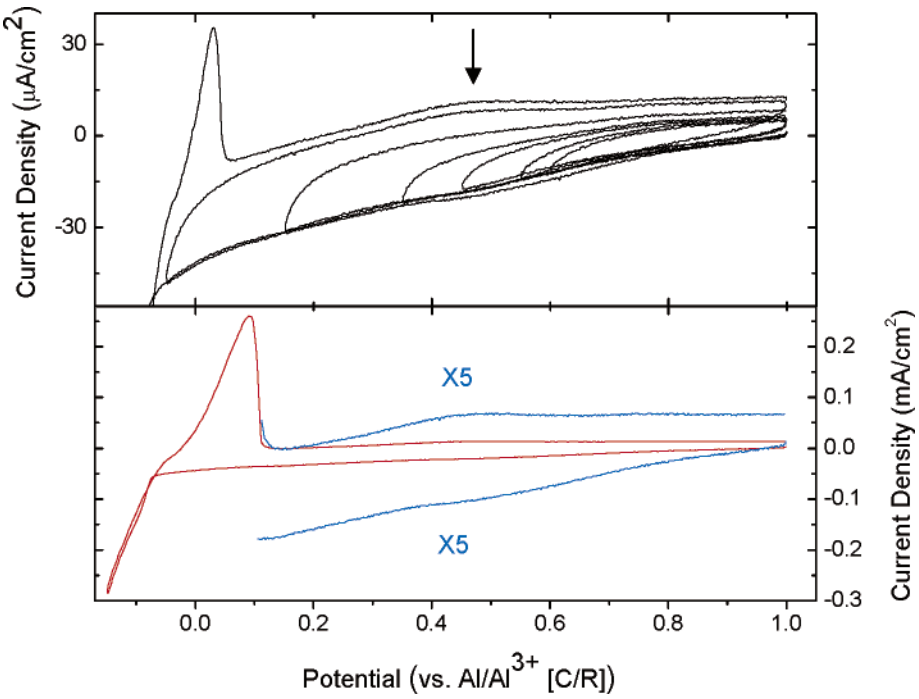

Figure 5. Series of cyclic voltammograms recorded at a scan rate of 20 mV/s for a W electrode prepared and characterized in UHV in $AlCl_3$/EtMeImCl (N = 1.1) at room temperature in the range $-0.15 < E < 1.0$ V (upper panel). This sequence was initiated at 1.0 V in the negative direction extending in each cycle the negative limit by of 0.05 V. For clarity, only a few of these curves are displayed in this figure. The last cycle of this sequence, i.e., $-0.15 < E < 2.0$ V, including an expansion of the curve in the y axis in the UPD region (X5) is given in the lower panel in this figure (see text for details).

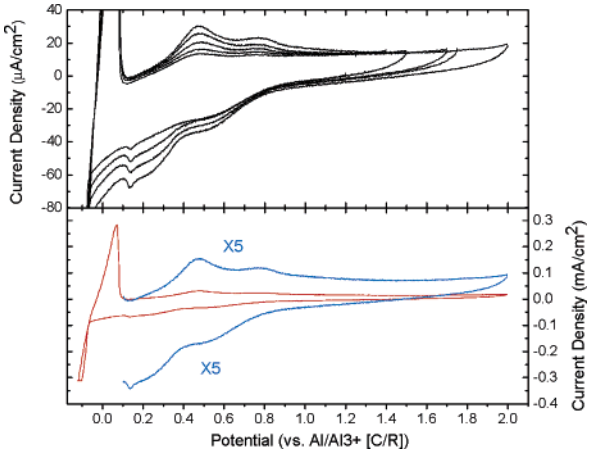

Figure 6. Series of cyclic voltammograms (scan rate = 20 mV/s) for the same W electrode prepared and characterized in UHV in $AlCl_3$/EtMeImCl ($N = 1.1$) recorded immediately after the sequence shown in Figure 5 had been completed. In this case the lower limit, i.e., −0.15 V, was kept fixed and the positive limit was extended in steps of 0.05 V. For clarity, only a few of these curves are displayed in this panel. The last cycle (not shown in the upper panel) is given in the lower panel, where the current in the UPD region has been expanded (X5) to enhance the features therein.

1.0 V. These data are displayed in the upper panel in Figure 5, where, for clarity, only a few of the cycles have been included. Also shown in this figure (see lower panel) is the voltammogram of the last cycle in this series, which exhibits prominent Al bulk deposition and stripping features, as well as the same curve only in the Al UPD region in expanded form (X5). Once this sequence was completed, a series of analogous window-opening experiments was initiated starting at 1.0 V in the positive direction in steps of 0.05 V up to 2.0 V keeping a fixed negative limit at −0.15 V (see upper panel, Figure 6), where, once again, only every other cycle was included in the graph. As in Figure 5, the last cycle in this series (and the corresponding expanded UPD region) is shown in the lower panel in this figure. A number of interesting observations can be made from a careful inspection of these data:

(i) The current observed immediately following polarization at 1.0 V was negligibly small. On extending the negative limit beyond the onset of Al bulk deposition, a rather broad peak centered at about 0.3 V was found in the subsequent scan in the positive direction (see arrow), in addition to Al bulk deposition stripping. This peak, attributable to underpotential stripping, was observed without any treatment positive to the initial potential. As evident from these results, the observed nucleation overpotential for Al bulk deposition was only a few tens of millivolts.

(ii) As the potential limit of the voltammetric scan in the positive direction was extended beyond 1.0 V (see Figure 6), the amplitude of the features attributed to Al UPD and stripping in the range, $0.10 < E < 0.75$ V increased significantly. Coulometric analysis of these features, using extensions of the currents in the purely capacitive region as baselines, yielded a common value of ca. 0.72 mC/cm^2. On the basis of crystallographic parameters, the average atom density for the low index faces of W is ca. 1×10^{15} atoms/cm^2. By assumption of 1 electron per W atom, this is equivalent to a charge density of 0.17 mC/cm^2; hence, the full discharge of Al^{3+} assuming one Al atom per W atom corresponds to ca. 0.59 mC/cm^2 or 1.2 monolayers, which compares well with other values reported in the literature.

(iii) The sequence of voltammetric curves in the range $1.0 < E < 2.0$ V (see upper panel, Figure 6) are rather featureless and thus consistent with the interface displaying mostly (double-layer) capacitive behavior (see below), i.e., no faradaic contributions. Also noteworthy is the increase in the magnitude of the capacitive current following each voltammetric cycle, which is indicative of a corresponding increase in the actual area of the electrode. On these bases, it may be concluded that the most reasonable explanation for the increase in the magnitude of the UPD features is a roughening of the W surface induced by the deposition and stripping of Al. This suggested model may also account for the earlier reports of Robinson and Osteryoung,[14] who noted that UPD features could only be observed following extensive potential cycling in the Al bulk deposition and stripping region. As mentioned briefly in the Introduction, Al UPD features on W for experiments involving the same melt performed in a glovebox have been observed upon cycling the electrode to potentials high enough (<2.5 V) for chlorine evolution to ensue[15] a procedure believed to remove oxides from the metal surface. Since no significant oxygen was detected by AES in our measurements prior to contacting the W surface with the melt and the potential scans were never extended beyond 2 V, it is very doubtful this type of *electrochemical cleaning* of the surface would be responsible for the emergence of clearly defined Al UPD features. Somewhat ironically the very low vapor pressure of the melt made it very difficult to remove the droplet of electrolyte left upon emersing the electrode at the end of the experiments; hence, no advantage could be taken of surface analytical techniques available in our UHV chamber to examine the surface following these experiments.

(iv) As mentioned above, the interfacial behavior in the range $1.0 < E < 1.8$ V resembles that of a simple capacitor. In fact, assuming that the surface is smooth, the specific capacity for the W−$AlCl_3$/EtMeImCl interface was found to be ca. 250 μF/cm^2. This value is higher than that found for the Au−$AlCl_3$/EtMeImCl interface during previous studies carried out in a glovebox with an inert atmosphere[17,18] but quite comparable to that found for Au in this study.

The extraordinarily low vapor pressure of the melt used for the experiments reported in this work opens new prospects for the study of the behavior of metals prepared and characterized in UHV in the strict absence of surface impurities. In addition to metal UPD and bulk deposition of pure metals and alloys other than Al, fundamental aspects of the structure and properties of well-defined single-crystal metal−ionic liquid interfaces could be investigated including the effect of impurities on the voltammetric behavior.

Acknowledgment. Work at CWRU and UM was supported in part by the U.S. Department of Energy, Office of Basic Energy Sciences.

References and Notes

(1) Hussey, C. L. *Pure and Appl. Chem.* **1988**, 1763. Wilkes, J. S.; Levisky, J. A.; Wilson, R. A.; Hussey, C. L. *Inorg. Chem.* **1982**, *21*, 1263−1264. Hussey, C. L. In *Chemistry of Nonaqueous Solutions: Current Progress*; Mamantov, G., Popovs, A. I., Eds.; New York, 1994; p 225.

(2) Papageorgiou, N.; Athanassov, Y.; Armand, M.; Bonhôte, P.; Pettersson, H.; Azam, A.; Grätzel, M. *J. Electrochem. Soc.* **1996**, (*10*), 3099−3108.

(3) Lewandowski, A.; Galinski, M. *J. Phys. Chem. Solids* **2004**, (*2*−*3*), 281−286.

(4) Li, Q. F.; Bjerrum, N. J. *J. Power Sources* **2002**, (*1*), 1−10.

(5) Liao, Q.; Pitner, W. R.; Stewart, G.; Hussey, C. L.; Stafford, G. R. *J. Electrochem. Soc.* **1997**, (*3*), 936−943.

(6) Lai, P. K.; Skyllas-Kazacos, M. *Electrochim. Acta* **1987**, (*10*), 1443−1449.

(7) Zell, C. A.; Endres, F.; Freyland, W. *Phys. Chem. Chem. Phys.* **1999**, (*4*), 697−704.; Zell, C. A.; Freyland, W. *Chem. Phys. Lett.* **2001**, (4−6), 293−298.

(8) Xu, X. H.; Hussey, C. L. *J. Electrochem. Soc.* **1992**, (*5*), 1295−1300.

(9) Hurley, H.; Weir, T. P. J. *J. Electrochem. Soc.* **1951**, 207.

(10) Carlin, T.; Crawford, W.; Bersch, M. *J. Electrochem. Soc.* **1992**, (*10*), 2720−2727.

(11) Stafford, G. R.; Hussey, C. L. Electrodeposition of Transition Metal-Aluminum Alloys from Chloroaluminate Molten Salts. In *Advances in Electrochemical Science and Engineering*; Alkire, R. C., Kolb, D. M., Eds. Wiley-VCH: Weinheim, 2002; Vol. 6.

(12) Lee, J. J.; Bae, I. T.; Scherson, D. A.; Miller, B.; Wheeler, K. A. *J. Electrochem. Soc.* **2000**, (*2*), 562−566. Lee, J.-J.; Mo, Y.; Scherson, D. A.; Miller, B.; Wheeler, K. A. *J. Electrochem. Soc.* **2001**, (*12*), C799−C802.

(13) Lee, J. J.; Miller, B.; Shi, X.; Kalish, R.; Wheeler, K. A. *J. Electrochem. Soc.* **2000**, (*9*), 3370−3376.

(14) Robinson, J.; Osteryoung, R. A. *J. Electrochem. Soc.* **1980**, (*1*), 122−128.

(15) Hamm, U. W.; Kramer, D.; Zhai, R. S.; Kolb, D. M. *J. Electroanal. Chem.* **1996**, (*1*), 85−89.

(16) Reniers, F. *J. Phys. D* **2002**, (*21*), R169−R188. Reniers, F.; Rooryck, V.; Pace, S.; Buess-Herman, C. *Surf. Interface Anal.* **2002**, (*1*), 623−627.

(17) Wang, K. L.; Chottiner, G. S.; Scherson, D. A. *J. Phys. Chem.* **1992**, (*16*), 6742−6744. Wang, K. L.; Chottiner, G. S.; Scherson, D. A. *J. Phys. Chem.* **1993**, (*39*), 10108−10111.

(18) Soriaga, M. P. *Prog. Surf. Sci.* **1992**, (*4*), 325−443.

(19) Stamenkovic, V.; Arenz, M.; Blizanac, B. B.; Mayrhofer K. J. J.; Ross, P. N.; Markovic, N. M. *Surf. Sci.* **2005**, (*576*), 145−157. Arenz, M.; Stamenkovic, V.; Ross, P. N.; Markovic, N. M. *Surf. Sci.* **2004**, (*573*), 57−66. Arenz, M.; Stamenkovic, V.; Schmidt, T. J.; Wandelt, K.; Ross, P. N.; Markovic, N. M. *Surf. Sci.* **2002**, (*506*), 287−296.

(20) Kunze, J.; Strehblow, H. H.; Staikov, G. *Electrochem. Commun.* **2004**, (*2*), 132−137. Foelski, A.; Kunze, J.; Strehblow, H. H. *Surf. Sci.* **2004**, (554), 10−24. Keller, P.; Strehblow, H. H. *Corros. Sci.* **2004**, (*8*), 1939−1952.

(21) Li, L. F.; Totir, D.; Gofer, Y.; Chottiner, G. S.; Scherson, D. A. *Electrochim. Acta* **1998**, (*6*−*7*), 949−955. Li, L. F.; Totir, D.; Chottiner, G. S.; Scherson, D. A. *J. Phys. Chem. B* **1998**, (*41*), 8013−8016.

(22) Tierney, B. J.; Pitner, W. R.; Mitchell, J. A.; Hussey, C. L. *J. Electrochem. Soc.* **1998**, (*9*), 3110−3116. Xu, X.-H.; Hussey, C. L. *J. Electrochem. Soc.* **1993**, (*5*), 1226−1233.